Cost Efficient Frequency Hopping Radar Waveform for Range and Doppler Estimation

Benjamin Nuss[1], Johannes Fink[2], Friedrich Jondral[2]

[1]Institut für Hochfrequenztechnik und Elektronik (IHE)
[2]Communications Engineering Lab (CEL)
Karlsruhe Institute of Technology (KIT), Germany
E-mail: benjamin.nuss@kit.edu, johannes.fink@kit.edu, friedrich.jondral@kit.edu

***Abstract*—A simple and cost efficient frequency hopping radar waveform which has been developed to be robust against mutual interference is presented. The waveform is based on frequency hopping on the one hand and Linear Frequency Modulation Shift Keying (LFMSK) on the other hand. The signal model as well as the radar signal processing are described in detail, focusing on the efficient estimation of range and Doppler of multiple targets in parallel. Finally, the probability of interference is estimated and techniques for interference mitigation are presented showing a good suppression of mutual interference of the same type of radar.**

I. Introduction

In recent years more and more radar systems in unlicensed bands have come to market resulting in an increasing interference level. Thus, new waveforms have to be developed being robust against mutual interference. Furthermore, in order to successfully compete in the market, the radars have to be cheap and thus, the hard- and software have to be as simple and cost efficient as possible. A well known and widely used radar waveform in automotive and automation markets is Linear Frequency Modulation Shift Keying (LFMSK) [1] which forms the basis of the developed frequency hopping radar waveform. It is based on a proposal in [2] where the author suggests to scramble the linear increasing frequency steps of LFMSK correspondent to a random permutation. However, this method leads to some problems in a dynamic scenario with multiple moving targets. To overcome these difficulties, especially the signal processing part of the waveform has been extended.

This paper is organized as follows: In Section II the frequency hopping signal is presented followed by the radar signal processing techniques in Section III. Section IV presents some analytical aspects as well as simulation results of the proposed radar system.

II. Signal Model

The radar signal is a modified version of a LFMSK signal where the linear increasing frequency steps are replaced by a random permutation of these steps. This results in a frequency hopping like signal where the hopping sequence is a random permutation π of length N, where N is the number of different steps. Thus, the probability that two independent radar systems chose exactly the same sequence π is given by

$$P(\Pi = \pi) = \frac{1}{N!} \ . \tag{1}$$

The height of one step is $\Delta f = \frac{B}{N}$, where B is the total occupied bandwidth of the frequency hopping signal. Each possible frequency is transmitted exactly once due to the random permutation. Fig. 1 shows an exemplary hopping sequence for $N = 1024$ and $B = 150\,\mathrm{MHz}$.

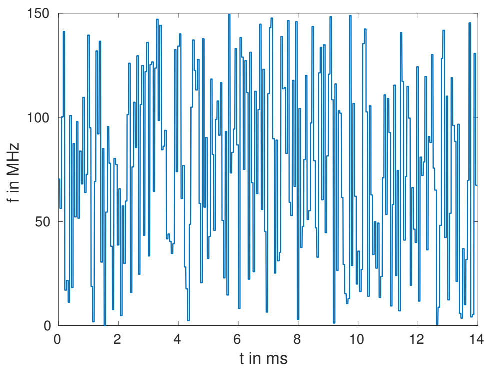

Fig. 1. Exemplary frequency hopping sequence of the proposed waveform

The analytical transmit (Tx) signal can be described as a sum of complex oscillations of the particular length $\frac{T}{N}$ and the frequency $f(n) = \frac{B}{N}\pi(n)$,

$$s(t) = A_{\mathrm{Tx}} \sum_{n=0}^{N-1} e^{\mathrm{j}2\pi\left(f_{\mathrm{c}}+\frac{B}{N}\pi(n)\right)t} \cdot \mathrm{rect}\left(\frac{t-\frac{T}{N}n}{\frac{T}{N}}\right) \ , \tag{2}$$

where T is the duration of the whole radar signal, f_{c} is the carrier frequency, $\pi(n)$ is the n-th number of the permutation and $\mathrm{rect}(t)$ the rectangular function defined in [3].

The receive (Rx) signal is an attenuated, time and frequency shifted version of the Tx signal. In the case of multiple targets, the reflected signals of all N_{t} objects are superimposed at the receiver resulting in

$$\begin{aligned} r(t) = &\sum_{i=1}^{N_{\mathrm{t}}} A_{\mathrm{Rx},i} \sum_{n=0}^{N-1} e^{\mathrm{j}2\pi\left(f_{\mathrm{c}}+\frac{B}{N}\pi(n)\right)\left(t-\frac{2\cdot(R_i-v_i\cdot t)}{c}\right)} \cdot \\ &\mathrm{rect}\left(\frac{t-\frac{R_i-v_i\cdot t}{c}-\frac{T}{N}n}{\frac{T}{N}}\right) \ . \end{aligned} \tag{3}$$

The down converted and low pass filtered Rx signal is sampled at a sampling rate of $f_\mathrm{s} = \frac{N}{T}$ correspondent to LFMSK. Thus, from each frequency step only one sample is taken resulting in a total of N complex values. The sampling point is chosen at the end of each step due to the settling time of the oscillator after each frequency hop in order to avoid transients. Neglecting the rectangular functions, the sampled baseband signal is given by

$$x(n) = \sum_{i=1}^{N_\mathrm{t}} A_i \cdot e^{-\mathrm{j}2\pi \frac{2f_\mathrm{c}R_i}{c}} \cdot e^{\mathrm{j}2\pi \frac{2v_i}{c}\left(f_\mathrm{c}+\frac{B}{N}\pi(n)\right)\frac{T}{N}n} \cdot e^{-\mathrm{j}2\pi \frac{B}{N}\pi(n)\frac{2R_i}{c}} \ . \tag{4}$$

Assuming that the bandwidth is much smaller than the carrier frequency, $B \ll f_\mathrm{c}$, (4) can be simplified to

$$x(n) \approx \sum_{i=1}^{N_\mathrm{t}} A_i \cdot e^{-\mathrm{j}2\pi \frac{2f_\mathrm{c}R_i}{c}} \cdot e^{\mathrm{j}2\pi \frac{2f_\mathrm{c}v_iT}{c}\frac{n}{N}} \cdot e^{-\mathrm{j}2\pi \frac{2R_iB}{c}\frac{\pi(n)}{N}} \ . \tag{5}$$

III. Radar Processing

For simplification the signal processing is outlined initially for a single target scenario. Further on also the case of multiple targets is treated. If only one target with no Doppler ($v = 0$) is considered, (5) can be rewritten to

$$x(n) = \underbrace{A \cdot e^{-\mathrm{j}2\pi \frac{2f_\mathrm{c}R}{c}}}_{=A'} \cdot e^{-\mathrm{j}2\pi \frac{2RB}{c}\frac{\pi(n)}{N}} \ . \tag{6}$$

The first exponential term is just a constant phase offset and can be combined with A to the complex amplitude A' whereas the second term can be used to extract the range information. Therefore, the samples are reordered according to the permutation sequence used on Tx side. Using the relation $\pi^{-1} \circ \pi = \pi \circ \pi^{-1} \equiv \mathrm{id}$, where id is the identity function, the reordered signal is given by

$$x^{\mathrm{ord}}(n) = x\left(\pi^{-1}(n)\right) = A' \cdot e^{-\mathrm{j}2\pi \frac{2RB}{c}\frac{n}{N}} \ , \tag{7}$$

where the second exponential term shows a linear increasing phase. Thus, an IFFT can be used to estimate the range of the target by determining the maximum of the IFFT spectrum.

However, if the target is moving, the Rx signal is frequency shifted by a Doppler offset. This results in a linear increasing phase term in $x(n)$ as it can be seen in (5). After reordering the samples, on the one hand the second term shows a linear phase, but on the other hand the linearity of the first term is destroyed resulting in a noise like spectrum. To avoid this, the Doppler shift has to be eliminated before reordering the samples. One possibility would be to estimate the frequency offset by an additional constant CW tone emitted before each hopping sequence. However, this would increase the duration of one Tx cycle and possibly be susceptible for interference. Additionally, multiple targets can have different Doppler shifts and thus the frequency offsets have to be assigned unambiguously to the different distances of these targets. To overcome these disadvantages multiple frequency offsets are eliminated in parallel regardless of the real Doppler shifts of the targets. Therefore, the sampled baseband signal is described by a vector $\mathbf{x} = [x(0)\ x(1)\ \ldots\ x(N-1)]$ of length N which allows all following signal processing steps to be written in matrix vector notation. To eliminate a frequency offset, this vector has to be multiplied element-wise with a complex cosine signal of the same length and the negative Doppler shift. Because multiple Doppler shifts shall be removed in parallel, a matrix $\mathbf{X} \in \mathbb{C}^{N \times N}$ is formed consisting of N-times the vector $\mathbf{x}$:

$$\mathbf{X} = \begin{pmatrix} \mathbf{x} \\ \vdots \\ \mathbf{x} \end{pmatrix} \ . \tag{8}$$

An efficient way to perform the elimination in parallel is to multiply $\mathbf{X}$ element-wise with a DFT-matrix $\mathbf{W}_N$,

$$\widetilde{\mathbf{X}} = \mathbf{X} \circ \mathbf{W}_N \ . \tag{9}$$

Here,

$$\mathbf{W}_N = \begin{pmatrix} 1 & \mathrm{e}^{-\mathrm{j}2\pi\frac{\left(-\frac{N}{2}\right)\cdot 1}{N^2}} & \ldots & \mathrm{e}^{-\mathrm{j}2\pi\frac{\left(-\frac{N}{2}\right)\cdot(N-1)}{N^2}} \\ 1 & \mathrm{e}^{-\mathrm{j}2\pi\frac{\left(-\frac{N}{2}+1\right)\cdot 1}{N^2}} & \ldots & \mathrm{e}^{-\mathrm{j}2\pi\frac{\left(-\frac{N}{2}+1\right)\cdot(N-1)}{N^2}} \\ \vdots & \vdots & \ddots & \vdots \\ 1 & \mathrm{e}^{-\mathrm{j}2\pi\frac{\left(\frac{N}{2}-1\right)\cdot 1}{N^2}} & \ldots & \mathrm{e}^{-\mathrm{j}2\pi\frac{\left(\frac{N}{2}-1\right)\cdot(N-1)}{N^2}} \end{pmatrix} . \tag{10}$$

is a vertically shifted version of the original DFT-matrix [4]. Thus, the frequency offset of zero appears at row index $m = \frac{N}{2}$, $m \in \{0, \ldots, N-1\}$. Furthermore, the vertical axis directly corresponds to the velocity axis.
Afterwards, the columns of $\widetilde{\mathbf{X}}$ have to be reordered according to the inverse permutation:

$$\widetilde{\mathbf{X}}^{\mathrm{ord}}(m,n) = \widetilde{\mathbf{X}}(m, \pi^{-1}(n)) \ . \tag{11}$$

To get the range axis, for each row of $\widetilde{\mathbf{X}}^{\mathrm{ord}}(m,n)$ an IFFT has to be calculated, resulting in

$$\widetilde{\mathbf{X}}^{\mathrm{ord}}(m,k) = \mathrm{IFFT}\left\{\widetilde{\mathbf{X}}^{\mathrm{ord}}(m,n)\right\} \ . \tag{12}$$

To detect the targets, a threshold γ can be applied, identifying all values with $\widetilde{\mathbf{X}}^{\mathrm{ord}}(\hat{m},\hat{k}) \geq \gamma$ to be a target, whose range and velocity can be directly estimated from the two-dimensional (2D) radar image. Fig. 2 shows an example with to targets at $20\,\mathrm{m}$ and $25\,\mathrm{m}$ and velocities of $-48\,\mathrm{km/h}$ and $16\,\mathrm{km/h}$.

The separation of multiple targets is possible due to the sum orthogonality within the IFFT. Only the reflected signal that corresponds to the actual frequency offset that is corrected shows a linear increasing phase after the correction resulting in a peak after the IFFT. This can be seen if we consider the case $f_{\mathrm{D},1} = \frac{2f_\mathrm{c}v_1}{c} = \frac{l}{T}$, where $f_{\mathrm{D},1}$ is the Doppler shift of target 1:

$$\begin{aligned}\widetilde{\mathbf{X}}^{\mathrm{ord}}(m=l,n) = &\\ & A_1' \cdot e^{\mathrm{j}2\pi \underbrace{\left(\frac{2f_\mathrm{c}v_1T}{c}-l\right)}_{=0}\frac{\pi^{-1}(n)}{N}} \cdot e^{-\mathrm{j}2\pi\frac{2R_iB}{c}\frac{n}{N}} + \\ & \sum_{i=2}^{N_\mathrm{t}} A_i' \cdot e^{\mathrm{j}2\pi \underbrace{\left(\frac{2f_\mathrm{c}v_iT}{c}-l\right)}_{\neq 0}\frac{\pi^{-1}(n)}{N}} \cdot e^{-\mathrm{j}2\pi\frac{2R_iB}{c}\frac{n}{N}} \ .\end{aligned} \tag{13}$$

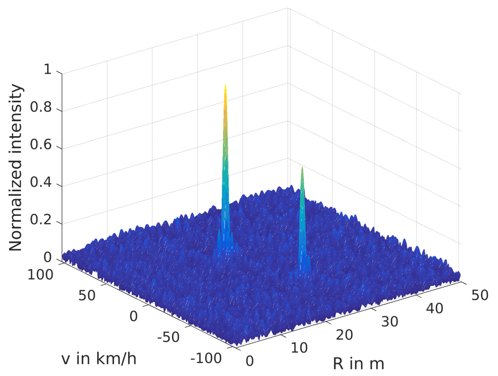

Fig. 2. 2D Radar image with 2 targets

The Doppler shift of target 1 is corrected whereas the remaining frequency offsets of the other targets lead to scrambled phase terms after the inverse permutation. Thus, after calculating the IFFT,

$$\widetilde{\mathbf{X}}^{\mathrm{ord}}(m=l,k) = A_1' \cdot \underbrace{\frac{1}{N}\sum_{n=0}^{N-1} e^{-\mathrm{j}2\pi\frac{2R_iB}{c}\frac{n}{N}} \cdot e^{\mathrm{j}2\pi\frac{nk}{N}}}_{=1 \text{ for } k=\frac{2R_iB}{c}} +$$

$$\sum_{i=2}^{N_t} A_i' \cdot \underbrace{\frac{1}{N}\sum_{n=0}^{N-1} e^{\mathrm{j}2\pi\left(\frac{2f_cv_iT}{c}-l\right)\frac{\pi^{-1}(n)}{N}} \cdot e^{-\mathrm{j}2\pi\frac{2R_iB}{c}\frac{n}{N}} \cdot e^{\mathrm{j}2\pi\frac{nk}{N}}}_{\approx 0}, \tag{14}$$

a peak only appears at the Doppler and range of the correspondent target. In the spectrum of the signals of all other targets with different Doppler shifts the random phase distribution after reordering the samples leads to a destructive superposition of the exponential terms.

In order to get a better velocity accuracy and to reduce the straddle loss a finer frequency grid can be chosen for the correction matrix $\mathbf{W}$. Then $\mathbf{W}$ is spanned by the dimensions $M \times N$ with $M \geq N$ and $\Delta f = \frac{f_s}{M}$. However, the velocity resolution itself stays unaffected. The range resolution can also be increased by zero padding which is done after the element-wise multiplication to avoid the unnecessary multiplication with zeros. Thus, only the computational effort of the IFFT increases but not the number of element-wise multiplications between $\mathbf{X}$ and $\mathbf{W}$.

IV. Simulation Setup and Results

A simulation setup consisting of one target and one interferer of the same radar type and the parameters as shown in Table I is done in MATLAB. A single point target at a distance of $R = 50\,\mathrm{m}$ is considered with a radar cross section of $\sigma = 10\,\mathrm{m}^2$. The figures are normalized in such a way that the target peak of this object has a height of $0\,\mathrm{dB}$ after the IFFT. The interference and the reflected signal from the target have the same power level to illustrate the interference mitigation effects.

TABLE I
Radar Parameters

Symbol	Parameter	Value
f_c	Carrier frequency	$24\,\mathrm{GHz}$
B	Total signal bandwidth	$150\,\mathrm{MHz}$
N	Number of frequency steps	1024
T	Signal duration	$14\,\mathrm{ms}$
ΔR	Range resolution	$\frac{c}{2B} = 1\,\mathrm{m}$
$R_{\max}$	Maximum unambiguous range	$N \cdot \Delta R = 1024\,\mathrm{m}$
Δv	Velocity resolution	$\frac{c}{2f_cT} = 0.45\,\mathrm{m/s}$
$v_{\max}$	Maximum unambiguous velocity	$\pm\frac{N}{2} \cdot \Delta v = \pm 229\,\mathrm{m/s}$

A. Probability of interference

The bandwidth B is divided into N equally spaced steps. Each frequency step is chosen once in every Tx cycle but the position is random. However, the interference occurs only at the steps, where the actual Tx frequencies of the two independent systems coincide. The probability that the random permutations of these two systems coincide in exactly k out of N steps can be derived using the Rencontres numbers, mentioned in [5]. In general, the Rencontres number $D_{N,k}$ describes the number of permutations of length N that have exactly k fixed points. Thus, with a number of $N!$ different permutations in total, the probability that two different hop sequences coincide in exactly k positions is given by

$$P(X=k) = \frac{D_{N,k}}{N!} = \frac{1}{k!} \cdot \sum_{i=0}^{N-k} \frac{(-1)^i}{i!}\,. \tag{15}$$

For an increasing number of permutation sets N the probability distribution can be approximated by a Poisson distribution with the expected value $\mu = \lambda = 1$ as shown in Fig. 3. Furthermore, it can be seen, that the probability for a collision of more than 4 frequency hops is lower than 0.4 %.

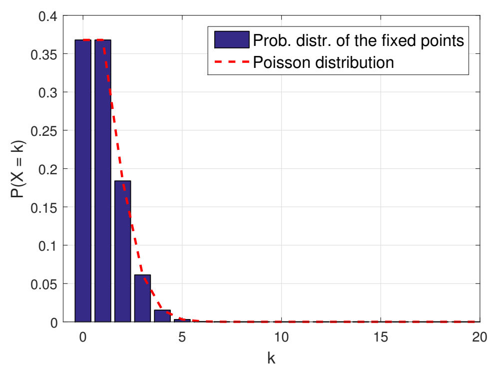

Fig. 3. Probability P, that two random permutations coincide exactly in k out of $N = 1024$ points

B. Interference Mitigation

The interference mitigation is based on two different effects: on the one hand the scrambling of the interfering hop sequence and on the other hand due to the low pass filtering when the two hop sequences differ. Fig. 4 shows the IFFT of the sampled baseband signals of the reflected and the interfering signal (both $v = 0$) before reordering the samples correspondent to the hop sequence of the transmitter. Both signals overlap in exactly one frequency step and have the same Rx power to illustrate directly the interference mitigation. As it can be seen in Fig. 4(a) the mean spectral power is the same before reordering and without filtering. When applying a low pass filter with a cutoff frequency of $f_{\mathrm{cut}} = \frac{f_s}{2 \cdot N}$, the interfering signal is attenuated. The remaining power results mainly from all frequency steps that coincide and thus are not filtered out. Also frequency steps from the interfering and the reflected signal that are close together can have some influence due to the limited filter order. However, this effect can be mitigated by higher filter orders with the disadvantage of higher hardware cost.

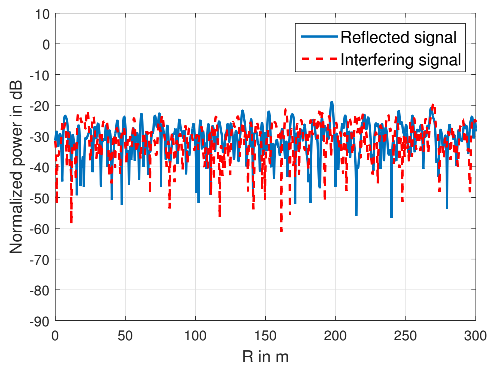

(a) without low pass filtering

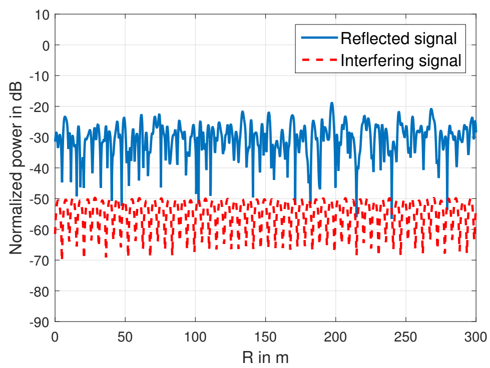

(b) with low pass filtering

Fig. 4. Power spectrum of the reflected and the interfering signal before reordering the samples ($f_{\mathrm{D}} = 0$)

After reordering the baseband samples a peak at $R = 50\,\mathrm{m}$ can be seen in the IFFT in Fig. 5(a). The attenuation of the interfering signal is due to the sum orthogonality that has been mentioned in Section III and shows a factor of approximately $10 \cdot \log_{10} N = 30\,\mathrm{dB}$. By low pass filtering the Rx signals before reordering the samples the interference mitigation is limited to a theoretical factor of $20 \cdot \log_{10} \frac{N}{N_{\mathrm{match}}}$, where N_{match} is the number of coinciding frequency steps. However, in order to achieve this factor an ideal low pass filter would be necessary. Due to the second interference mitigation effect by the inverse permutation the filter order can be reduced without reducing the interference suppression too much. Thus, also the complexity and the hardware cost can be reduced.

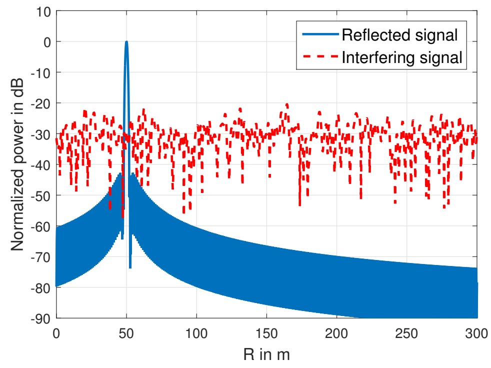

(a) without low pass filtering

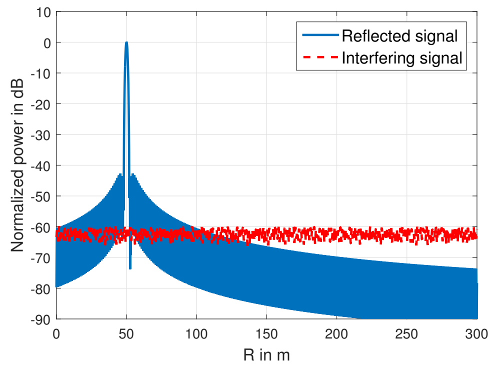

(b) with low pass filtering

Fig. 5. Power spectrum of the reflected and the interfering signal after reordering the samples ($f_{\mathrm{D}} = 0$)

V. Conclusion

A simple interference robust radar waveform has been proposed with the capability to estimate range and Doppler of multiple targets simultaneously. The signal processing steps haven been outlined and the methods for interference mitigation have been described in detail and illustrated in an example. The result shows a good reduction of the interference power after the signal processing for interfering radars of the same type but different random hop sequences.

VI. Acknowledgements

This work has been performed during the author's master thesis at the Communications Engineering Lab (CEL) at the Karlsruhe Institute of Technology in 2015.

References

[1] M.-M. Meinecke, M. A. Obojski, and J. Knaup, "Increasing vehicular safety at intersections by using LFMSK modulated radar sensors," in *Radar Symposium (IRS), 2010 11th International*, June 2010, pp. 1–4.
[2] M. Jankiraman, N. Willis, and H. Griffiths, *Design of multi-frequency CW radars*. SciTech Pub., 2007.
[3] R. Bracewell, *The Fourier Transform and Its Applications*, ser. Electrical engineering series. McGraw Hill, 2000.
[4] V. K. Ingle and J. G. Proakis, *Digital Signal Processing Using MATLAB*, 3rd ed. CENGAGE Learning Custom Publishing, 2011.
[5] A. Camina, *An Introduction to Enumeration*, ser. Springer Undergraduate Mathematics Series, B. Lewis, Ed. Springer London, 2011.